

Muons as probes of dynamical spin fluctuations: some new aspects

Amit Keren

Department of Physics, Technion—Israel Institute of Technology, Haifa 32000, Israel
and
Rutherford Appleton Laboratory, Chilton Didcot, Oxfordshire OX11 0QX, UK

E-mail: keren@physics.technion.ac.il

Received 5 August 2004

Published

Online at stacks.iop.org/JPhysCM/16/1

doi:10.1088/0953-8984/16/0/000

Abstract

This paper describes the impact of dynamic spin fluctuations on the muon spin relaxation signal in the longitudinal field set-up, namely, when a field is applied along the initial muon spin direction. Our main objective is to show that the μ SR technique can do more than determine the correlation time of the spins in the system under investigation. It can, in fact, determine if the concept of correlation time is valid to begin with, and if not suggest alternatives. Consequently, the paper shows what to expect from the muon signal over a range of situations starting from a simple antiferromagnetic hopping model to more complicated models involving power laws and other types of correlation functions. The application of all models to experimental data is demonstrated. The possibility that the muon, by itself, generates dynamic fluctuations is critically examined by comparing muon and neutron scattering data.

(Some figures in this article are in colour only in the electronic version)

1. Introduction

One of the biggest advantages of the muon spin relaxation technique (μ SR) as a probe of magnetism is the fact that muons are produced and injected into the sample 100% polarized. As a consequence, no field is needed to achieve polarization and the technique can operate even in zero field (ZF). If, and when, a field is applied in the direction parallel to the muon polarization it is for completely different reasons. This field probes frequency dependent properties of the magnetic system under investigation. Due to this ZF capability, the field, and hence the frequency, can be varied over several orders of magnitude. The limitations come only from the ability to zero the external field, or from internal undesired field sources such as nuclear moments. This property of μ SR leads to serious challenges for analysis since the data

[See endnote 1](#)

Processing

JPC/cm184710/SPE: [MuSR](#)

Printed 13/8/2004

[Focal Image](#)

(Ed: SARAH)

CRC data

File name	First page
Date req.	Last page
Issue no.	Total pages
Artnum	Cover date

do not always agree with the very natural and intuitive concept of correlation time, or even with a distribution of correlation times. Addressing this challenge is the main purpose of this paper. It will be done in three steps:

- (I) we demonstrate how the muons detect dynamic fluctuations,
- (II) we show that they are an honest probe and do not alter these fluctuations, and
- (III) we examine cases where the concept of correlation time must be relaxed and replace it with other concepts.

The paper is therefore organized as follows: section 2 provides a simple model for muon behaviour in a dynamic magnetic environment, which could be solved analytically with no approximations. The model teaches us how to extract dynamic information in all cases where the static polarization is known either theoretically or experimentally, and will serve as a test case for more complicated models, which could only be solved approximately. We also demonstrate the experimental application of this model. In section 3 we derive an approximate, yet analytical, relation between the field dependent muon spin relaxation $[T_1^{-1}(H)]$ and the correlation time. This will also be demonstrated experimentally. In section 4 we show that the muon does not change the dynamics it detects by comparing the measured T_1^{-1} in MnF_2 with the spectral density determined from inelastic neutron scattering on the same system. Finally, in section 5 we show experimental situations where the concept of correlation time breaks down, and exotic correlation functions must be invoked. The μSR signal in this situation will be discussed and once again demonstrated experimentally. Concluding remarks will be given in section 6.

2. A solvable model of dynamic fluctuations

Our solvable model considers a field at the muon site \mathbf{B} exactly perpendicular to the $\hat{\mathbf{z}}$ direction, which flips with time between the up and down directions but maintains its absolute value. The $\hat{\mathbf{z}}$ direction is taken to be the initial muon spin direction and also the direction in which the polarization is measured. As a result the muon spin rotates with frequency $\pm\omega$. The polarization resulting from three such field flips is demonstrated in figure 1.

This can happen if a sample is an antiferromagnet (AFM) and the muon hops between different sites of opposite fields. We assume that the field fluctuation could be described by a flip rate probability per unit time ν . We further define ν_t as the total hop rate. If each time the muon hops it has the same chance of experiencing a field change as not experiencing a field change then

$$\nu = \nu_t/2. \quad (1)$$

This assumption is called the strong collision approximation, and will only apply if the muon hops over long distances compared to the unit cell. For a discussion of the relaxation rate in this situation without the strong collision approximation (and arbitrary field distribution) see [1]. In our situation the field correlation function after the short interval $d\tau$ is given by

$$\langle B(d\tau)B(0) \rangle = B^2 \left(1 - \frac{\nu_t}{2} d\tau \right) - B^2 \frac{\nu_t}{2} d\tau = B^2(1 - \nu_t d\tau)$$

where $\langle \rangle$ stands for the average. As can be proven by induction, after time τ

$$\langle B(\tau)B(0) \rangle = B^2 \exp(-\nu_t \tau). \quad (2)$$

Thus the field correlation function decays exponentially with a correlation time of $1/\nu_t$.

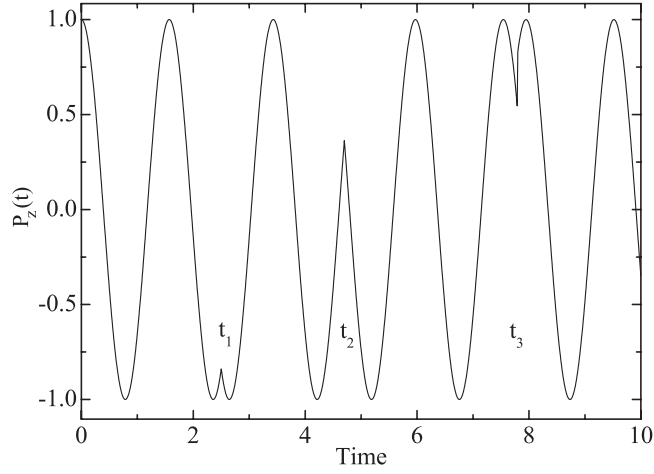


Figure 1. A demonstration of the muon polarization in the \hat{z} (initial) direction in the antiferromagnetic model in which the field flips but maintains its magnitude. In this figure three field flips are taking place.

For n hops between sites of opposing fields, at times $t_1 < \dots < t_n < t$, the polarization function g_n is given by

$$g(t_1, \dots, t_n, t) = \text{Re} \exp\left(i \sum_{j=1}^{n+1} [-1]^{j+1} \omega [t_j - t_{j-1}]\right) \quad (3)$$

where $t_{n+1} = t$. In this form it is clear that

$$g(t_1, \dots, t_n, t) = \text{Re} \prod_{j=1}^{n+1} g_j(t_j - t_{j-1}) \quad (4)$$

where

$$g_j(t_j - t_{j-1}) = \exp([-1]^{j+1} i \omega [t_j - t_{j-1}]).$$

Next we calculate the probability that a field flip will occur at a time t_{i+1} , given that a previous change occurred at time t_i . For this we divide the time segment $t_{i+1} - t_i$ into m steps each dt long and take $m \rightarrow \infty$. This gives the probability

$$\lim_{m \rightarrow \infty} \left[1 - v \frac{t_{i+1} - t_i}{m}\right]^m v dt = e^{-v(t_{i+1} - t_i)} v dt.$$

Therefore, the probability for n field flips in the time segments $[t_1, t_1 + dt_1], \dots, [t_n, t_n + dt_n]$ is

$$\prod_{i=1}^n \exp[-v(t_i - t_{i-1})] v dt_i = v^n \exp(-vt) \prod_{i=1}^n dt_i.$$

The averaged polarization is obtained by taking the sum over all possible numbers of field flips, weighted by their probability, and integrating over the times in which they can take place [2]. This leads to

$$P_z^{\text{AFM}}(t) = e^{-vt} g(t) + v e^{-vt} \int_0^t dt_1 g(t_1, t) + v^2 e^{-vt} \int_0^t dt_2 \int_0^{t_2} dt_1 g(t_1, t_2, t) + \dots \quad (5)$$

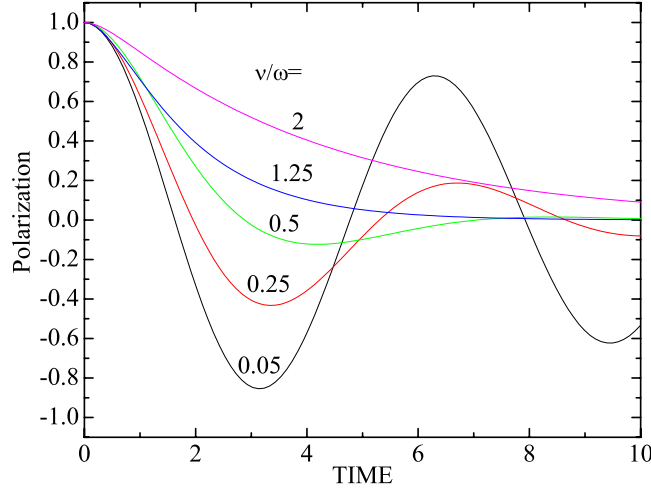


Figure 2. The expected muon spin polarization in the antiferromagnetic model for various ratios of flip rates to oscillation frequency.

where $g_n(t_1, \dots, t_n, t)$ is given by (3). In the simple case presented here the series could be summed [3] and it leads to

$$P_z^{\text{AFM}}(t) = c_+ e^{z_+ t} + c_- e^{z_- t} \quad (6)$$

where

$$c_{\pm} = \frac{1}{2} \pm \frac{v(v^2 - \omega^2)^{-\frac{1}{2}}}{2}$$

and

$$z_{\pm} = -v \pm (v^2 - \omega^2)^{\frac{1}{2}}.$$

Note that this result is correct regardless of the strong collision approximation of equation (1).

The polarization P_z^{AFM} for selected values of v/ω is shown in figure 2. Clearly, as the field flip rate increases the oscillations at frequency ω disappear. When $v/\omega \rightarrow \infty$ the muon behaves as if it experiences zero field, which is the average field. Another important aspect of this model, which we will refer to later, is that when $v \gg \omega$ and the strong collision assumption (equation (1)) is adopted, the polarization could be approximated by

$$P_z^{\text{AFM}}(t) = \exp\left(-\frac{\gamma_{\mu}^2 B^2}{\nu_t} t\right) \quad (7)$$

giving a simple relation between the relaxation rate and the correlation function.

In figure 3 we present the application of this model to a powder sample of the antiferromagnetic compound $\text{Ca}_{0.86}\text{Sr}_{0.14}\text{CuO}_2$ [3]. This compound has a Néel temperature of 540 K, and at a temperature of 360 K the electronic moments reach 90% of their full frozen size [4]. Yet the muon spin precession is not seen until a temperature of 245 K, as depicted in figure 3. This is associated with muon diffusion at high temperatures [3]. The data in figure 3 are fitted to

$$P_z(t) = A_1 \exp(-t/T_1) + A_2 \exp(-t/T_2) P_z^{\text{AFM}}(\omega, \nu, t). \quad (8)$$

The parameters A_1 and A_2 are introduced since the field in the powder is not perpendicular to \hat{z} . The relaxation times T_1 and T_2 account for field distribution and relaxation mechanisms other

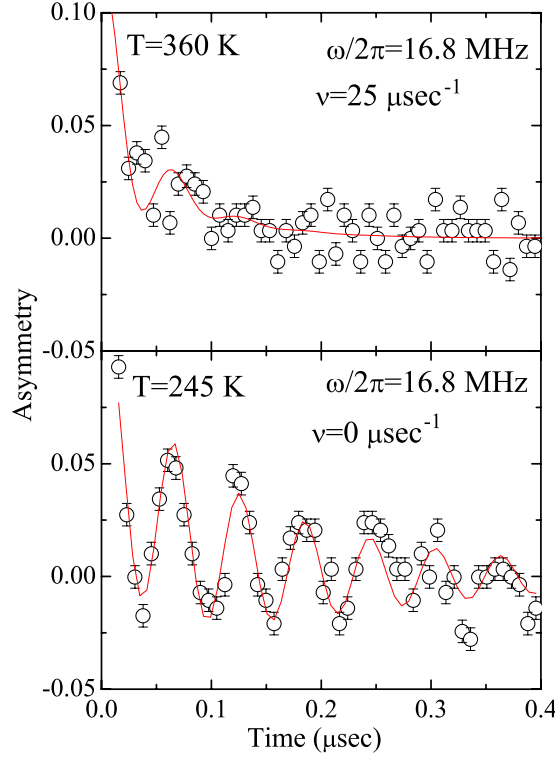


Figure 3. Asymmetry in the antiferromagnet $\text{Ca}_{0.86}\text{Sr}_{0.14}\text{CuO}_2$ at two temperatures well below T_N . The fit at $T = 245$ K, demonstrated by the solid curve, is to equation (8) with $\nu = 0$. The solid curve at $T = 360$ K is obtained using the same equation and parameters as for $T = 245$ K, but with $\nu = 25 \mu\text{s}^{-1}$.

than hopping. The fit at 240 K is done with $\nu = 0$ to determine all other parameters. It gives $\omega/2\pi = 16.8$ MHz. The fit at the temperature of 360 K is obtained simply by substituting $\nu = 25$ MHz in equation (8) (using the 245 K values for all other parameters).

When in the presence of a longitudinal field or more complicated field distributions, numerical methods must be applied. For this purpose it is useful to write the infinite series of equation (5) in a compact form

$$P_z(\nu, t) = e^{-\nu t} g(t) + \nu \int_0^t dt' P_z(\nu, t - t') e^{-\nu t'} g(t'). \quad (9)$$

This is known as the Volterra equation of the second kind and it can be solved numerically [5]. To verify the equivalence between equations (9) and (5), we first note that the first term on the rhs of equation (9) is the same as the first term equation (5). Next we generate a sister equation to (9) by substituting $t' \rightarrow t''$ followed by $t \rightarrow t - t'$ in this equation. Finally, we replace $P_z(\nu, t - t')$ under the integral in equation (9) by the sister equation. This leads to

$$P_z(\nu, t) = e^{-\nu t} g(t) + \nu e^{-\nu t} \int_0^t dt' g(t - t') g(t') + \dots$$

if $g(t_1, t) = g(t - t_1)g(t_1 - 0)$ (strong collisions), so that now both the first and the second terms on the rhs of equations (9) and (5) agree. Repeating this operation on equation (9) will regenerate equation (5).

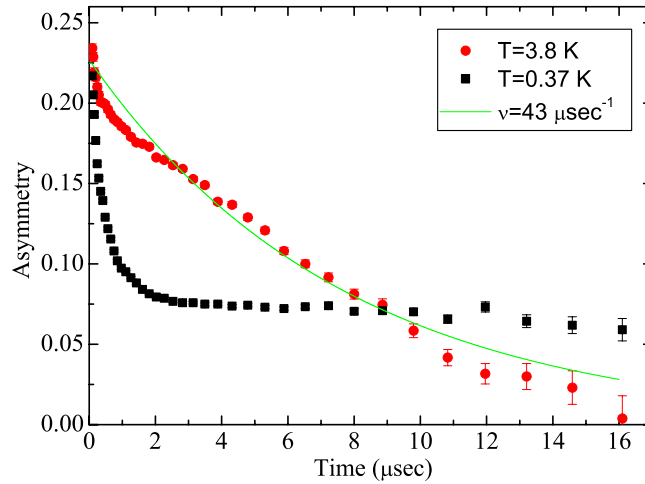


Figure 4. Static ($T = 0.37$ K) and dynamic ($T = 3.8$ K) asymmetries in a compound with coexisting superconductivity and magnetism (symbols) [8]. The solid curve is the expected asymmetry taking the measured static asymmetry as $g(t)$, a fluctuation rate $\nu = 43 \mu\text{s}^{-1}$, and the Volterra equation (9).

The Volterra equation gives a good description of the dynamics only when the strong collision approximation, manifested in equation (4), is valid. All it needs to be solved is the input $g(t)$, which is the static function. Therefore, there are three ways of using equation (9) to obtain dynamic information. The first one is in simple cases where $g(t)$ is known analytically as was done by Brewer *et al* [6] for the F- μ -F bond. The second one is when $g(t)$ must be obtained numerically as in the cases of Gaussian [2] or Lorentzian [7] field distribution with external longitudinal field. The third way is to measure $g(t)$ by cooling the system to low enough temperatures that no dynamic fluctuations are present any longer, and to use the measured $g(t)$ in the Volterra equation. In figure 4 we present an attempt to do so. The data are taken from zero-field measurements in a compound where superconductivity and magnetism coexist [8]. At a temperature of 0.37 K the muon relaxation is completely static. This can be inferred from the fact that the relaxation is to a third of the initial asymmetry (on average a third of the muons experience a static field parallel to their initial polarization). However, this static relaxation function is unusual; the relaxation is overdamped whereas theories predict damped relaxation (with a dip before the constant part of $P_z(t)$). Despite the lack of theoretical explanation for the static relaxation, one can estimate the fluctuation rate at a temperature of 3.8 K using equation (9). The solid curve shows the result of this equation where $\nu = 43 \mu\text{s}^{-1}$ and with the input $g(t)$ taken from the $T = 0.37$ K data. This fit is not very good, but there is a lot to be learned from the discrepancy as well [8].

[See endnote 2](#)

3. Perturbation approach

Extracting dynamic information using the Volterra equation fails when the system cannot be described by a correlation time or when the strong collision approximation fails. Therefore, in this section we use a perturbation approach to extract dynamic information without making any assumptions about the field's time evolution. We follow the full quantum derivation given in [9]. A semi-classical treatment can be found in [10]. The Hamiltonian of the muon spin $I = 1/2$ experiencing both an external static longitudinal field (LF) H , and an internal

dynamically fluctuating field $\mathbf{B}^d(t)$ can be decomposed into

$$\mathcal{H} = \mathcal{H}_0 + \mathcal{H}'(t) \quad (10)$$

where

$$\mathcal{H}_0 = -\gamma_\mu \hbar I_z H \quad (11)$$

is the secular (time independent) part, and the interaction part is

$$\mathcal{H}' = -\gamma_\mu \hbar \mathbf{I} \cdot \mathbf{B}^d(t). \quad (12)$$

In this notation the spin operators have no dimensions. When the fluctuating fields are smaller than the external field we can use time dependent perturbation theory and write the time propagator as

$$U(t) = \exp\left(-\frac{i}{\hbar} \mathcal{H}_0 t\right) \left[1 - \frac{i}{\hbar} \int_0^t dt' \mathcal{H}'(t') - \frac{1}{\hbar^2} \int_0^t dt' \int_0^{t'} dt'' \mathcal{H}'(t') \mathcal{H}'(t'') + \dots \right] \quad (13)$$

where the perturbation Hamiltonian in the interaction picture is given by

$$\mathcal{H}^I(t) = \exp(i\mathcal{H}_0 t / \hbar) \mathcal{H}'(t) \exp(-i\mathcal{H}_0 t / \hbar). \quad (14)$$

This Hamiltonian simplifies to

$$\mathcal{H}^I(t) = -\gamma_\mu \hbar \mathbf{B}^d(t) \mathbf{I}^I(t) \quad (15)$$

where

$$\begin{aligned} I_x^I(t) &= I_x \cos(\omega t) + I_y \sin(\omega t) \\ I_y^I(t) &= I_y \cos(\omega t) - I_x \sin(\omega t) \\ I_z^I(t) &= I_z \end{aligned} \quad (16)$$

and

$$\omega = \gamma_\mu H.$$

Note that $\mathbf{I}^I(t)$ is the time-dependent spin operator in the interaction picture, namely, of a muon that rotates around the external field as if there were no internal fields. Mathematically this leads to oscillations in the LF data at the frequency of the external field as we shall see shortly.

The polarization of a muon at a given site as a function of time $P_z(t)$ is given by

$$P_z(t) = \text{Tr}[\rho U^\dagger(t) I_z U(t)] \quad (17)$$

where $\rho = 1 + 2P_0 I_z$ and P_0 is the initial polarization. If we now write

$$P_z(t) = P_0 \exp(-\Gamma(t)t), \quad (18)$$

expand this equation in powers of Γ , and compare it with equation (17), we find [9]

$$\Gamma(t)t = \frac{\gamma_\mu^2}{4} \int_0^t d\tau (t - \tau) [e^{i\omega\tau} \Phi_{+-}(\tau) + e^{-i\omega\tau} \Phi_{-+}(\tau)] \quad (19)$$

where

$$\Phi_{ij}(t' - t'') = \langle B_i(t') B_j(t'') + B_j(t'') B_i(t') \rangle,$$

$B_\pm = B_x \pm iB_y$, $B_i(t)$ denotes the i th spatial component of the time dependent fluctuating field, and $\langle \rangle$ stands for thermal and sample averages. When the fields are taken as classical objects and correlations between orthogonal directions are ignored, then equation (19) simplifies to

$$\Gamma(t)t = \gamma_\mu^2 \int_0^t d\tau (t - \tau) \Phi(\tau) \cos(\omega\tau) \quad (20)$$

where

$$\Phi(t' - t'') = \langle B_x^d(t') B_x^d(t'') + B_y^d(t') B_y^d(t'') \rangle. \quad (21)$$

However, in order to connect $\Gamma(t)t$ to electronic spin fluctuation, rather than field fluctuation, the full quantum treatment must be retained. At late times, such that $\Phi(\tau)$ is negligible, one finds that

$$\lim_{t \rightarrow \infty} \Gamma(H, t) = \frac{1}{T_1(H)} = \gamma_\mu^2 \int_0^\infty \Phi(\tau) \cos(\omega\tau) d\tau. \quad (22)$$

Therefore T_1^{-1} is approximately the cosine transform of the field correlation function.

Next we examine the same correlation function as in

$$\Phi(\tau) = 2(\Delta^2/\gamma_\mu^2) \exp(-\nu|\tau|) \quad (23)$$

where Δ/γ_μ is the RMS of the instantaneous field distribution, and ν is the inverse correlation time. After the integration of equations (20) with (23) we find [11]

$$\Gamma(H, t)t = \frac{2\Delta^2}{(\omega^2 + \nu^2)^2} \{ [\omega^2 + \nu^2]\nu t + [\omega^2 - \nu^2][1 - e^{-\nu t} \cos(\omega t)] - 2\nu\omega e^{-\nu t} \sin(\omega t) \}. \quad (24)$$

We can see from this formula that, in general, the polarization relaxes; however, some oscillations of frequency ω exist near $\nu t \rightarrow 0$. Since equation (13) is an expansion in products of the internal magnetic field, which is on the scale of Δ , and time, which is on the scale of $1/\nu$, it is an expansion in Δ/ν and equation (24) is expected to be a good approximation for $\Delta/\nu < 1$. We also expect equation (19) to give an accurate account of the relaxation at $\nu t < 1$ since the n th term in equation (13) involves n integrations in time, and its contribution is proportional to the volume of integration $(\nu t)^n$. The requirements on the parameter ν prevent us from taking the limits $\nu \rightarrow 0$ and $t \rightarrow \infty$ simultaneously. Therefore, in the perturbation theory we cannot discuss the static limit at long times. In the fast fluctuation limit $\nu \gg \omega$ we find

$$\Gamma(H, t) = \frac{1}{T_1} = \frac{2\Delta^2\nu}{\omega^2 + \nu^2}. \quad (25)$$

In zero external field ($\omega = 0$) this result agrees with the equation (7) of the AFM model up to a factor of two, provided that here ν is interpreted as a total fluctuation rate. The factor of two is due to the fact that here both x and y direction fluctuations contribute whereas in equation (7) only one direction is active.

A successful application of equation (24) to a real experimental data set was performed by Carreta *et al* in [12] with the frustrated two-dimensional $S = 1/2$ Heisenberg antiferromagnet $\text{Li}_2\text{VOSiO}_4$. This compound has both a fast fluctuating component and a slow one. Accordingly they fit their data by multiplying equation (18) (with equation (24)) by $\exp(-\lambda t)$. The muon polarization and their fit are depicted in figure 5. The fit is impressively good over more than two orders of magnitude of the applied field, yielding $\gamma_\mu\Delta = 0.65 \mu\text{s}^{-1}$ and $\nu = 3.774 \mu\text{s}^{-1}$.

4. From field to spin fluctuations

While equation (22) is well known and often used to interpret μSR experiments, one would still like to make sure that the muon does not change the correlation function Φ . In this section we show that the muon $1/T_1$ in the ordered state ($T < T_N$) of the antiferromagnet MnF_2 can be accounted for by the sum of host spin fluctuations measured by neutron scattering. For

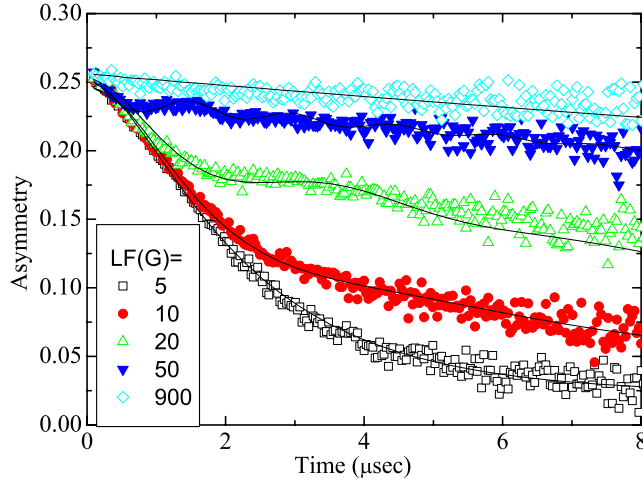


Figure 5. Demonstration of the application of equation (18) with equation (24) to the frustrated magnet $\text{Li}_2\text{VOSiO}_4$ [12].

this discussion we first adopt Moriya's [13] ideas originally developed for nuclear magnetic resonance (NMR) and apply them in our case. The starting point is the breaking of the electronic spins into two parts: static and dynamic, namely,

$$\mathbf{S}^j = \langle \mathbf{S}^j \rangle + \delta \mathbf{S}^j \quad (26)$$

where $\langle \mathbf{S}^j \rangle$ is the time average of the j th spin, and $\delta \mathbf{S}^j$ is its fluctuating part. The static part of the field \mathbf{B}^s emerges from $\langle \mathbf{S}^j \rangle$ and serves as H in the above derivation. The dynamic part \mathbf{B}^d stems from $\delta \mathbf{S}^j$. In MnF_2 , \mathbf{B}^s coincides with the easy $\hat{\mathbf{c}}$ axis and both can be aligned with the initial polarization [14].

The muon-spin to electronic-spin interacting Hamiltonian could be written as

$$\mathcal{H}_{\text{int}} = \gamma_\mu \hbar \sum_j \mathbf{I} \cdot \mathbf{A}_j \cdot \mathbf{S}_j \quad (27)$$

which means that the dynamic field experienced by the muons is

$$\mathbf{B}^d = - \sum_j \mathbf{A}_j \cdot \delta \mathbf{S}_j. \quad (28)$$

It is customary to introduce the Fourier transform in the space of the spin variable. In MnF_2 there is only one magnetic ion per unit cell, and we can define

$$\mathbf{S}^{\mathbf{k}} = N^{-1/2} \sum_j \mathbf{S}^j \exp(i\mathbf{k} \cdot \mathbf{R}^j). \quad (29)$$

Combining equations (19), (28), and (29) gives

$$1/T_1 = (1/2N) \sum_{\mathbf{k}} \sum_{\kappa\kappa'} D_{\kappa\kappa'}(\mathbf{k}) \int_{-\infty}^{\infty} d\tau \cos(\omega_s \tau) \{ \delta S_{\kappa}^{\mathbf{k}}(\tau), \delta S_{\kappa'}^{-\mathbf{k}}(0) \} \quad (30)$$

where $\{ \}$ stands for the anti-commutator. $D_{\kappa\kappa'}(\mathbf{k})$ (given in [15]) is a form factor determined by the Fourier transform of the coupling \mathbf{A}_j . We do not provide an explicit expression for this factor since we will shortly make a simplifying assumption. Most of the contribution to the sum in equation (30) is from \mathbf{k} near the staggered magnetization wavevector \mathbf{k}_0 of the antiferromagnetic order. We therefore define $\mathbf{q} = \mathbf{k} - \mathbf{k}_0$. Since \mathbf{A}_j is very short range, as

a function of j , and since the correlation function peaks at $q = 0$ [16], we can approximate $D_{\nu\nu'}(\mathbf{q})$ as independent of q for small q . Similar approximations were used by De Renzi *et al* [16] in their work on μ SR line width in MnF_2 at $T > T_N$. In the most general case, both longitudinal and transverse spin fluctuations contribute to $1/T_1$. But the longitudinal fluctuations in MnF_2 do not contribute to $1/T_1$, as we shall demonstrate experimentally, and only S_x and S_y should be considered. Using the definition of the neutron scattering function

$$S_{\perp}(\mathbf{q}, \omega) = \int_{-\infty}^{\infty} dt \cos(\omega t) \langle \{ \delta S_{\perp}^{\mathbf{q}}(t), \delta S_{\perp}^{-\mathbf{q}}(0) \} \rangle \quad (31)$$

we arrive at

$$\frac{1}{T_1}(T) = D \int S_{\perp}^{\text{T}}(\mathbf{q}, \omega_s(T)) d^3q \quad (32)$$

where D is a constant independent of temperature, $\omega_s = \gamma_{\mu} B^s$, and the sum over \mathbf{q} is replaced by an integral.

The temperature dependence of the rhs of equation (32) enters in two places: one is the temperature dependence of the scattering function $S_{\perp}^{\text{T}}(\mathbf{q}, \omega)$, and the other is the temperature dependence of the static local field $\omega_s(T)$, which is given formally by $-\gamma_{\mu} \sum_j \mathbf{A}_j \cdot \langle \mathbf{S}^j \rangle$ but in reality could be measured.

μ SR measurements in MnF_2 were performed by Uemura *et al* [14]. They used two experimental configurations in zero external field: (a) the transverse configuration (TC) in which the initial muon polarization was perpendicular to the $\hat{\mathbf{c}}$ axis and (b) the longitudinal configuration (LC) in which the initial polarization was parallel to $\hat{\mathbf{c}}$. In TC they measured the precession frequency of the muon moment in the static local field at $T < T_N$, and thus obtained $\omega_s(T)$. Two frequencies were found in the μ SR spectra and assigned to two different muon sites. In LC they measured the relaxation rate of the muon polarization at temperatures both above and below T_N . Here again two relaxation timescales were observed. The fast relaxation was attributed to muons at the high field site. We are concerned here only with the spin–lattice relaxation of muons in the site with the higher field since the data are less scarce. In figure 6 we show the fast $1/T_1$ as a function of temperature [14]. It is obvious from the figure that at temperatures higher than the Néel temperature $1/T_1$ is independent of T . This is clear evidence that $1/T_1$ is independent of the longitudinal spin fluctuation, since these fluctuations are known to undergo critical slowing down as discussed in [14, 17, 16].

Schulhof *et al* [17] measured the scattering function $S_{\perp}(\mathbf{q}, \omega)$ in MnF_2 by neutron scattering. They showed that near T_N $S_{\perp}(\mathbf{q}, \omega)$ could be approximated by

$$S_{\perp}(\mathbf{q}, \omega) \propto \frac{1}{\kappa_{\perp}^2 + \mathbf{q}^{*2}} \left(\frac{\Gamma_{\perp}}{\Gamma_{\perp}^2 + (\omega - \omega_0)^2} + \frac{\Gamma_{\perp}}{\Gamma_{\perp}^2 + (\omega + \omega_0)^2} \right) \quad (33)$$

where ω_0 and Γ_{\perp} are functions of the temperature and are given by

$$\begin{aligned} \omega_0(T, q) &= a_0(T) + b_0(T)(q^*)^2, \\ \Gamma_{\perp}(T, q) &= a_{\perp}(T) + b_{\perp}(T)(q^*)^2, \\ q^{*2} &= q_x^2 + q_y^2 + (c/a)^2 q_z^2, \end{aligned} \quad (34)$$

where a and c are the lattice constants. The parameters $\kappa_{\perp} = 0.054 \text{ \AA}^{-1}$, $a_0(T) = 1.36(1 - T/T_N)^{0.37} \text{ meV}$, $a_{\perp}^{-1}(T) = 7.52 + 164.3(1 - T/T_N)^{0.72} \text{ meV}^{-1}$, $b_0(T) = 15.6 + 23.8(1 - T/T_N)^{0.57} \text{ meV}$, and $b_{\perp}^{-1}(T) = 0.08 + 5 \times 10^{-4}(1 - T/T_N)^{2.54} (10^{-2} \text{ meV})^{-1}$ can be found in [15]. This form of $S_{\perp}(\mathbf{q}, \omega)$ and $\omega_s(T)$ is then used to numerically integrate the right-hand side of equation (32) at various temperatures. The integral was performed in a cube, and the range of integration was limited by the available neutron data ($q < 0.3 \text{ \AA}^{-1}$). The temperature dependence of this integral was then scaled by a factor D so that both sides

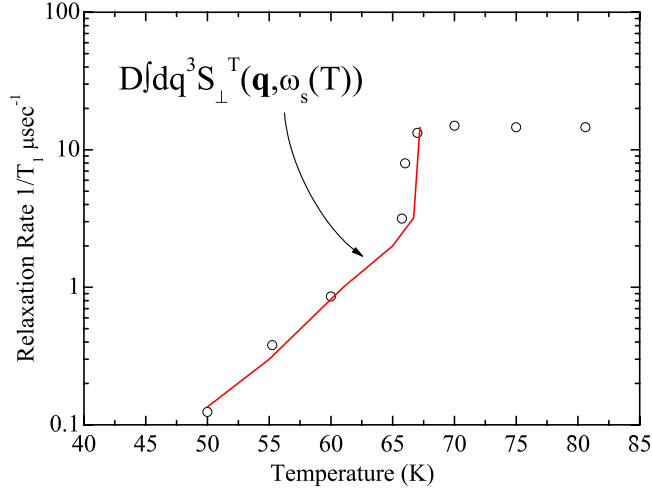


Figure 6. Temperature dependence of the muon T_1^{-1} at the high field site in MnF_2 . The solid line is a theoretical prediction of T_1^{-1} using the measured neutron scattering function $S(\mathbf{q}, \omega)$ in the same compound [17] and equations (33) and (34).

of equation (32) agree at T_N . The result of the computed $1/T_1$ is shown in figure 6 by the solid line. In this figure we can see that the calculated line agrees very well with the measured data. Indeed, the muon relaxation rate in the ordered state of MnF_2 results from host spin fluctuations according to equation (32) without any noticeable addition from the presence of the muon.

5. Exotic spin correlation

The need to postulate new types of correlation functions emerges from many experimental situations in which $T_1(H)$ is not a linear function of H^2 , as required by equation (25), despite the fact that the muon relaxes exponentially and T_1 is well defined. One example is the frustrated magnet $\text{Tb}_2\text{Ti}_2\text{O}_7$ [18]. Raw muon relaxation data at a temperature of 100 mK in this system are presented in the inset of figure 7 on a semi-log scale. Clear field dependence is observed. The solid line is a fit to exponential decay plus a small field independent background. The extracted T_1 versus H (taken from [18]) is presented in figure 7. Clearly T_1 is a linear function of H and not of H^2 .

Since $\text{Tb}_2\text{Ti}_2\text{O}_7$ shows many properties similar to those of a spin glass, the first strategy to try and explain these data is by postulating randomness as in a spin glass. In a standard spin glass, the muon could stop in a variety of environments and can experience different instantaneous fields or correlation times. If we allow for a distribution of Δ and/or ν we can obtain an average polarization \bar{P} by

$$\bar{P}(H, t) = \int \int \rho(\Delta, \nu) P \left(\frac{2\Delta^2 \nu t}{\nu^2 + (\gamma_\mu H)^2} \right) d\Delta d\nu.$$

Nevertheless, in the high field limit, namely, $\gamma_\mu H \gg \nu^{\max}$, where ν^{\max} is the highest fluctuation rate in the distribution, we still expect

$$\bar{P}(H, t) = \bar{P}(t/H^2).$$

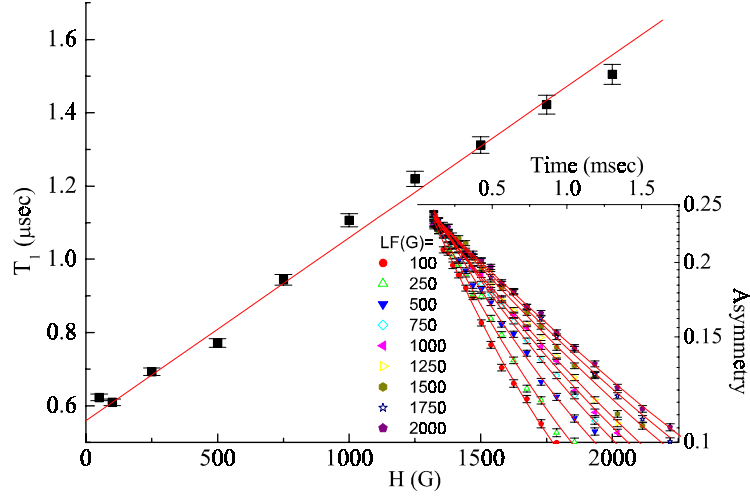


Figure 7. The muon relaxation time T_1 as a function of the longitudinal field H in the cooperative paramagnet $Tb_2Ti_2O_7$ showing linear field dependence. The inset shows the raw asymmetry as a function of time for various fields on a log scale demonstrating that the muon polarization decay is exponential.

Thus, even with randomness, the timescale of relaxation T_1 , at high fields, must depend on H^2 even when a distribution of Δ and/or ν are taken into account. In other words, a distribution of correlation times or field strengths, as suggested for spin glasses in [19] and [7] respectively, could not explain the data in figure 7.

Therefore, we examine the possibility of other correlation functions. Interesting candidates are a power law (PL)

$$\Phi(\tau) \sim c\tau^{-x}, \quad (35)$$

a stretched exponential (SE)

$$\Phi(\tau) \sim c \exp[-(\lambda\tau)^y], \quad (36)$$

or the cut-off power law (CPL), which is often approximated in computational physics by the Ogielski form (OF) [20]

$$\Phi(\tau) \sim c\tau^{-x} \exp[-(\lambda\tau)^y]. \quad (37)$$

Mathematical justification for these functions can be found in [21]. They are also applied for the analysis of neutron spin echo (NSE) experiments [22]. Using asymptotic expansion in terms of ω of equation (22) for the difference correlation functions we can predict the interplay between the field and time. It is possible to write for all three cases and high enough fields

$$P(H, t) = P(t/H^\gamma) \quad (38)$$

where [23]

$$\gamma = \begin{cases} 1-x & \text{PL} \\ 1-x & \text{OF} \\ 1+y & \text{SE} \end{cases}. \quad (39)$$

This is a good approximation for all values of x . It is also a good approximation for y not much smaller than unity but gets worse as y approaches zero. The new and exotic correlation functions open the way to understand the unusual $T_1(H)$.

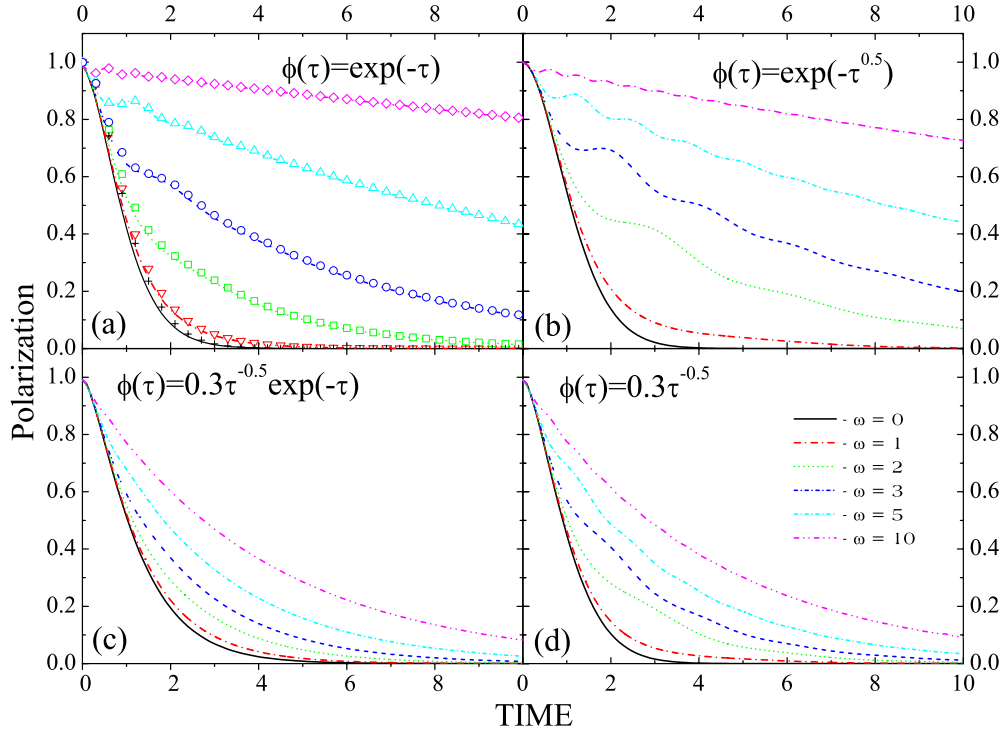


Figure 8. The muon spin polarization obtained numerically for different correlation functions and various longitudinal fields using equations (18) and (20).

However, for real data analysis one must normalize the PL and CPL so that they do not diverge at $\tau = 0$. One possibility for doing this normalization is to introduce a cut-off time τ_c so that in the most general case

$$q(\tau) = 2\Delta^2 \frac{\tau_c^x}{(\tau + \tau_c)^x} \exp[-(\nu\tau)^y]. \quad (40)$$

However, since τ_c is expected to be on the scale of 10^{-13} to 10^{-11} s, while the first point in time where the muon polarization is measured is typically at $t \simeq 10^{-8}$ s, the PL, SE, and CPL can be reconstructed from equation (40) with

$$c = 2\Delta^2 \tau_c^x.$$

To regain confidence in equations (38) and (39), we integrate equation (20) with the three correlation functions of equations (35)–(37) as an input using the ‘improper integration’ method described in [5]. The result is presented in figure 8 panels (a)–(d) where we show the expected muon polarization for $\Phi(\tau) = \exp(-\tau)$, $\exp(-\tau^{0.5})$, $0.3\tau^{-0.5}\exp(-\tau)$, and $0.3\tau^{-0.5}$ respectively, and various fields. The pre-factor in the correlation function c was chosen so that all relaxation rates are nearly identical at zero field. This allows us to compare the effectiveness of the field in decoupling the muon polarization. Clearly, the decoupling is harder in cases which involve a power law.

In figure 9 we demonstrate the scaling relations given by equation (38) for the different correlation functions given in figure 8. We find that they hold for high enough fields and late enough time. Thus, our numerical results demonstrate that the asymptotic expansion leading to equation (39) is indeed valid.

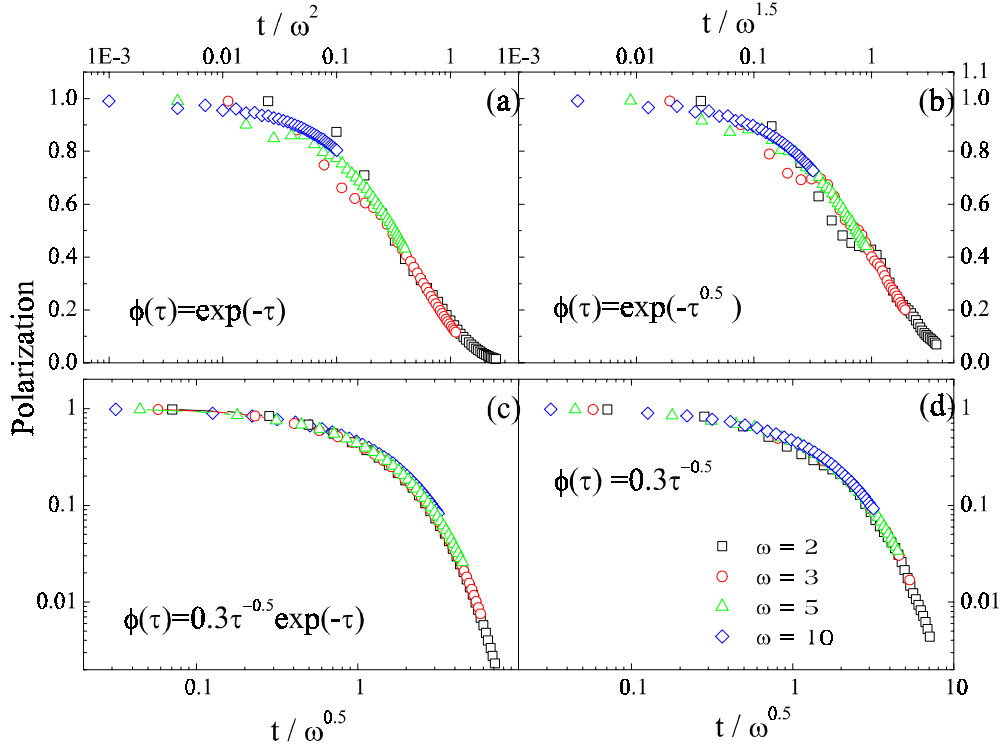


Figure 9. The same data as in figure 8 but plotted as a function of scaled time according to equations (38) and (39).

These scaling relations were demonstrated experimentally in the Ising spin glass $\text{Fe}_{0.05}\text{TiS}_2$ [24], and are reproduced here in figure 10. This compound has a T_g of 7.5 K. In this case the correlation function changes its nature from a CPL to an SE upon cooling as can be seen in the figure. At 20 K the polarization is a function of $t/H^{0.3}$ but at 8 K the scaling $t/H^{1.3}$ is more appropriate.

Other examples of scaling in non-spin-glass materials can be found in the paper of MacLaughlin *et al* [25], and a linear field dependent relaxation timescale was observed by Pratt *et al* [26]. Of course figure 7 is yet another demonstration of the scaling relation in which $\gamma = 1$. This could emerge from $x \rightarrow 0$ or $y \rightarrow 0$. However, since the asymptotic expansion breaks down for $y \rightarrow 0$, $\gamma = 1$ emerges as being most likely from $x \rightarrow 0$. This situation could be further analysed. Assuming that the correlation function is a PL, equation (22) gives

$$\frac{1}{T_1} = \frac{2\Delta^2(\gamma_\mu H \tau_e)^x}{\gamma_\mu H} \Gamma(1-x) \sin\left(\frac{\pi x}{2}\right). \quad (41)$$

Using the fact that for small $x \Gamma(1-x) \sin(x\pi/2) = x\pi/2 + O(x^2)$ we obtain

$$T_1(H) \simeq \frac{2\gamma_\mu H}{x\Delta^2} \quad (42)$$

resulting in a linear dependence between T_1 and H . To increase confidence in this equation we check if reasonable values for the theoretical parameters can produce the observed T_1 . For example if $\tau_e \sim 10^{-13}$ s, \mathbf{B}_\perp and H on the order of 100 G ($\gamma_\mu H \sim \Delta \sim 10$ MHz) and $x = 0.02$ obtained by NSE [18], we have $(\gamma_\mu H \tau_e)^x \sim 1$ and $T_1 \sim 1 \mu\text{s}$, on the order of the measured value. We thus believe that equation (42) describes the data in figure 7 appropriately.

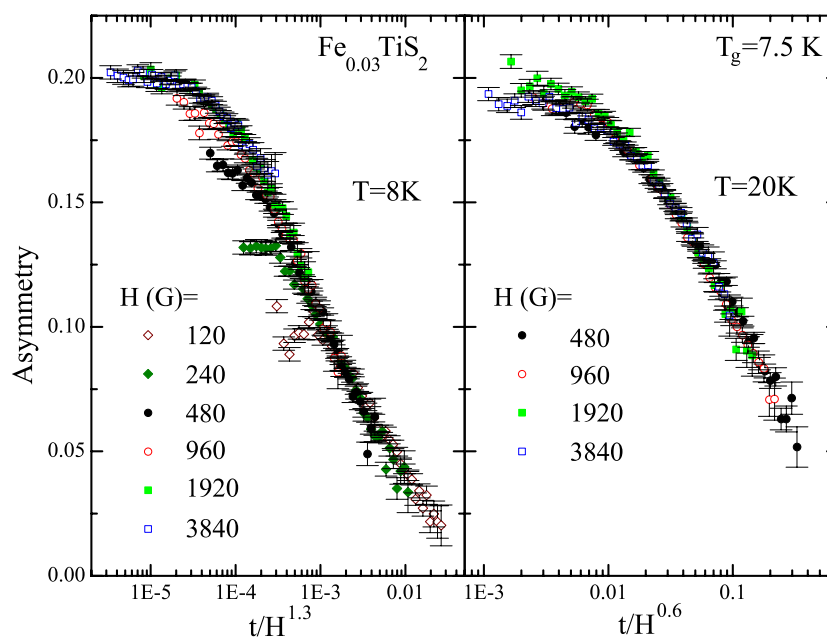


Figure 10. The asymmetry plotted in the Ising spin glass system $\text{Fe}_{0.03}\text{TiS}_2$ as a function of t/H^γ for a geometrical series of fields higher than 60 G. At $T = 20\text{K}$ all data sets collapse into one function for $\gamma = 0.6$. The same happens in $T = 8\text{K}$ provided that $\gamma = 1.3$.

6. Conclusions

We demonstrated that μSR in the longitudinal field configuration can be used to characterize the time dependent part of the spin dynamic auto-correlation function, and that the muon itself does not modify this function. The technique is capable of distinguishing between different types of behaviours, ranging from power law to stretched exponential decays, a property which until recently was associated only with NSE [27]. In some cases the two techniques agree [22, 25] on the nature of the correlation, in others they do not [25]. NSE is a more direct probe of the correlation function but requires high concentration of spins; μSR works in low concentration of magnetic spins and enjoys a relatively high counting rate. Thus correlation functions could be characterized within a few hours.

References

- [1] Klauder J R and Anderson P W 1962 *Phys. Rev.* **125** 912
- [2] Hayano R S, Uemura Y J, Imazato J, Nishida N, Yamazaki T and Kubo R 1979 *Phys. Rev. B* **20** 850
- [3] Keren A, Le L P, Luke G M, Sternlied B J, Wu W D, Uemura Y J, Tajima S and Uchida S 1993 *Phys. Rev. B* **48** 12926
- [4] Vaknin D, Caignol E, Davies P K, Fischer J E, Johnston D C and Goshorn D P 1989 *Phys. Rev. B* **39** 9122
- [5] Press W H, Flannery B P, Teukolsky A A and Vetterling W T 1989 *Numerical Recipes* (Cambridge: Cambridge University Press)
- [6] Brewer J H, Harshman D R, Keitel R, Kreitzman S R, Luke G M, Noakes D R and Turner R E 1986 *Hyperfine Interact.* **32** 677
- [7] Uemura Y J, Yamazaki T, Harshman D R, Senab M and Ansaldo E J 1985 *Phys. Rev. B* **31**
- [8] Kanigel A, Keren A, Eckstein Y, Knizhnik A, Lord S and Amato A 2002 *Phys. Rev. Lett.* **88** 137003
- [9] McMullen T and Zaremba E 1978 *Phys. Rev. B* **18** 3026

See endnote 3

-
- [10] Keren A, Bazalitsky G, Campbell I and Lord J S 2001 *Phys. Rev. B* **64** 054403
- [11] Keren A 1994 *Phys. Rev. B* **50** 10039
- [12] Carretta P, Melzi R, Papinutto N and Millet P 2002 *Phys. Rev. Lett.* **88** 047601
- [13] Moriya T 1962 *Prog. Theor. Phys.* **28** 371
- [14] Uemura Y J *et al* 1986 *Hyperfine Interact.* **31** 313
- [15] Keren A, Le L P, Luke G M, Wu W D and Uemura Y J 1994 *Hyperfine Interact.* **85** 363
- [16] De Renzi R, Guidi G, Podini P, Tedeschi R, Bucci C and Cox S F J 1984 *Phys. Rev. B* **30** 197
- [17] Schulhof M P, Nathans R, Heller P and Linz A 1971 *Phys. Rev. B* **4** 2254
- [18] Keren A, Gardner J S, Ehlers G, Fukaya A, Segal E and Uemura Y J 2004 *Phys. Rev. Lett.* **92** 107204
- [19] Campbell I A, Amato A, Gyax F N, Herlach D, Schenck A, Cywinski R and Kilcoyne S H 1994 *Phys. Rev. Lett.* **72** 1291
- [20] Ogielski T 1985 *Phys. Rev. B* **32** 7384
- [21] Sokolov I M, Klafter J and Blumen A 2002 *Phys. Today* (November) 55
Klafter J, Shlesinger M F and Zumofen G 1996 *Phys. Today* (February) 33
Metzler R and Klafter J 2000 *Phys. Rep.* **339** 1
- [22] Pappas C, Mezei F, Ehlers G, Manuel P and Campbell I A 2003 *Phys. Rev. B* **68** 054431
- [23] Keren A, Mendels P, Campbell I A and Lord J 1996 *Phys. Rev. Lett.* **77** 1386
- [24] Keren A, Gulener F, Campbell I, Bazalitsky G and Amato A 2002 *Phys. Rev. Lett.* **89** 107201
- [25] MacLaughlin D E, Bernal O O, Heffner R H, Nieuwenhuys G J, Rose M S, Sonier J E, Andraka B, Chau R and Maple M B 2001 *Phys. Rev. Lett.* **87** 066402
- [26] Pratt F L, Blundell S J, Hayes W, Nagamine K, Ishida K and Monkman A P 1997 *Phys. Rev. Lett.* **79** 2855
- [27] Mezei F and Murani A P 1979 *J. Magn. Magn. Mater.* **14** 211

[See endnote 4](#)

Queries for IOP paper 184710

Journal: **JPhysCM**
Author: **A Keren**
Short title: **Muons as probes**

Page 1

Query 1:-

Author: Please be aware that the colour figures in this article will only appear in colour in the Web version. If you require colour in the printed journal and have not previously arranged it, please contact the Production Editor now.

Page 6

Query 2:

Author: 'Voltera' changed to 'Volterra' in fig. 4 caption to match text—OK?

Page 15

Query 3:-

Author: [7]: Please provide page number.

Page 16

Query 4:-

Author: [21]: Please provide volume number of the first two references.